Blocking CXCL1-dependent neutrophil recruitment prevents immune damage and reduces pulmonary bacterial infection after inhalation injury

Julia L. M. Dunn,[1] Laurel B. Kartchner,[1] Wesley H. Stepp,[1,2] Lindsey I. Glenn,[1,2] Madison M. Malfitano,[1,2] Samuel W. Jones,[2,3] Claire M. Doerschuk,[4,5] 🅾 Robert Maile,[1,2,3,*] and Bruce A. Cairns[1,2,3,*]

[1]Department of Microbiology and Immunology, The University of North Carolina at Chapel Hill, Chapel Hill, North Carolina; [2]Department of Surgery, The University of North Carolina at Chapel Hill, Chapel Hill, North Carolina; [3]Jaycee Burn Center, The University of North Carolina at Chapel Hill, Chapel Hill, North Carolina; [4]Department of Medicine and Pathology, Center for Airway Disease, The University of North Carolina at Chapel Hill, Chapel Hill, North Carolina; and [5]Marsico Lung Institute, University of North Carolina at Chapel Hill, Chapel Hill, North Carolina

Dunn JL, Kartchner LB, Stepp WH, Glenn LI, Malfitano MM, Jones SW, Doerschuk CM, Maile R, Cairns BA. Blocking CXCL1-dependent neutrophil recruitment prevents immune damage and reduces pulmonary bacterial infection after inhalation injury. *Am J Physiol Lung Cell Mol Physiol* 314: L822–L834, 2018. First published January 25, 2018; doi:10.1152/ajplung.00272.2017.—Smoke inhalation associated with structural fires, wildfires, or explosions leads to lung injury, for which innovative and clinically relevant animal models are needed to develop effective therapeutics. We have previously reported that damage-associated molecular patterns (DAMPs) and anti-inflammatory cytokines correlate with infectious complications in patients diagnosed with inhalational injury. In this study, we describe a novel and translational murine model of acute inhalational injury characterized by an accumulation of protein and neutrophils in the bronchoalveolar space, as well as histological evidence of tissue damage. Mice were anesthetized, and a cannula was placed in the trachea and exposed to smoldering plywood smoke three times for 2-min intervals in a smoke chamber. Here we demonstrate that this model recapitulates clinically relevant phenotypes, including early release of double-stranded DNA (dsDNA), IL-10, monocyte chemoattractant protein (MCP)-1, and CXCL1 along with neutrophilia early after injury, accompanied by subsequent susceptibility to opportunistic infection with *Pseudomonas aeruginosa*. Further investigation of the model, and in turn a reanalysis of patient samples, revealed a late release of the DAMP hyaluronic acid (HA) from the lung. Using nitric oxide synthase-deficient mice, we found that Nos2 was required for increases in IL-10, MCP-1, and HA following injury but not release of dsDNA, CXCL1 expression, early neutrophilia, or susceptibility to opportunistic infection. Depletion of CXCL1 attenuated early neutrophil recruitment, leading to decreased histopathology scores and improved bacterial clearance in this model of smoke inhalation. Together, these data highlight the potential therapeutic benefit of attenuating neutrophil recruitment in the first 24 h after injury in patients.

acute lung injury; inhalation; neutrophil; woodsmoke

* R. Maile and B. A. Cairns contributed equally to this work.
Address for reprint requests and other correspondence: R. Maile, 3007D Burnett Womack Bldg., CB#7206, Dept. of Surgery, Univ. of North Carolina at Chapel Hill, Chapel Hill, NC 27599 (e-mail: robert_maile@med.unc.edu).

INTRODUCTION

Acute smoke inhalation injury presents a clinical challenge. Acute smoke inhalation occurs during structural fires or wildfires, which are increasing in number and size across the United States. According to statistics compiled by the Insurance Information Institute, 61,920 wildfires burned in the United States in 2016 compared with 58,225 in 2015. Over 10% of households are at extreme risk in Idaho, Colorado, California, New Mexico, Texas, and Utah, placing millions of households at extreme risk for smoke inhalation injury. Inhalational injuries result in severe and complex damage to the lung and are associated with lengthy and expensive hospitalizations, especially when they occur concomitantly with cutaneous burn injury (2). In cases where smoke inhalation is accompanied by cutaneous burns, lacerations, or fractures, inhalational injury is treated last, since it is dwarfed by the immediacy of these other traumatic injuries (37).

The short- and long-term physiological imbalances that result from acute smoke inhalation injury are not completely understood, in large part because a systematic analysis of patient outcomes is complicated by the confounding variables (e.g., cutaneous burns) that normally accompany inhalation injury. In addition, this patient population spans all ages, ethnicities, and comorbidities. Moreover, the severity of the inhalational injury depends on the smoke source, concentration, and duration of exposure. For example, synthetic materials often burn faster and release more toxins than wood; therefore, as synthetic materials become more prevalent in construction, the types of lung injuries treated at trauma centers become more diverse (37).

A leading cause of morbidity and mortality following inhalational injury is bacterial pneumonia, which is thought to be the result of poor mucociliary clearance coupled with impaired immunological surveillance (41). Some studies have examined patient bronchoalveolar lavage fluid (BALF) to characterize the inflammatory state, identify patients at risk for developing pneumonia, and thus initiate antibacterial prophylaxis in high-risk patients. Two damage-associated molecular patterns (DAMPs), double-stranded DNA (dsDNA) and hyaluronic

acid (HA), have been demonstrated to be elevated in patients with inhalational injury, especially those who subsequently develop bacterial pneumonia (29). In addition, our group has previously shown that IL-10 was elevated in patients who develop pulmonary or peripheral bacterial infections, and others have observed elevated IL-10 in patients who do not survive inhalational injury (10, 22). The prevailing opinion is that trauma leads to release of DAMPs that lead to a suppression of inflammation and contribute to patients' inability to fight opportunistic bacterial infections; however, we have not observed a direct correlation between the concentrations of DAMPs and IL-10 in patients. We therefore sought to develop a translational mouse model of inhalational injury to probe the relationship between local DAMP release in response to inhalation injury and short- and long-term local immune function as it relates to susceptibility to opportunistic infection.

Wood smoke inhalation elicits a clinically relevant injury model. A reliable small animal model of disease is an invaluable resource for identification of mechanism(s) to inform the development of and test the efficacy of therapeutic interventions. Several studies have used small (e.g., mice, rats) and large (e.g., sheep, pigs) animal models to address acute smoke inhalation, primarily using cotton as a source of smoke (15, 25, 26, 30, 33, 39, 42). Neutrophil accumulation and activation are associated with oxidative tissue damage in an ovine model of cotton smoke inhalation and bacterial infection (26). Inhibiting protein oxidation in a mouse model of cotton smoke inhalation with burn injury resulted in elevated IL-10 and an improvement in lung structure (15). Notwithstanding these insights, there are still significant differences between the clinical observations in humans and the results of animal studies, underlying the need for preclinical models that more closely mimic the clinical setting (15, 37). Despite differences in magnitude, innate immune responses to stressors are largely similar in humans and mice, including cytokine and chemokine production and leukocyte activation (9). Thus, in this study, we describe and use a novel murine model of acute exposure to smoke from plywood, a common building material comprised of wood and adhesives. This model uses a source of smoke that is more representative of the type of injury observed within burn centers, resulting in the recapitulation of many phenotypes previously described in patients diagnosed with an inhalational injury and key traits of murine lung injury. We employed this model to address the hypothesis that immune activation early after smoke inhalation injury leads to damage to the tissue architecture and inflammation, which renders the lung vulnerable to subsequent bacterial challenge. In addition, we establish the utility of this model for testing interventions that counteract the negative physiological consequences of smoke inhalation. Specifically, we report that exposure to wood smoke leads to accumulation of DAMPs (HA and dsDNA), elevated levels of IL-10, monocyte chemoattractant protein (MCP)-1, and CXCL1, and neutrophil accumulation in BALF. Furthermore, mechanistic studies demonstrate that Nos2 expression is necessary for injury-induced elevations in IL-10, MCP-1, and HA but not for changes in CXCL1, neutrophil recruitment, or the susceptibility to bacterial challenge. In contrast, CXCL1 neutralization results in an approximate 50% decrease in neutrophil recovery from the BALF following injury and improved bacterial clearance. Thus, this study establishes the utility of this model in determining mechanisms that drive this complex injury and highlights its suitability for testing interventions that counteract the negative physiological consequences of smoke inhalation.

MATERIALS AND METHODS

Mouse housing and care. Female (or male, where stated) C57BL/6 mice aged 8–10 wk were purchased from Taconic Farms and housed in specific pathogen-free facilities. All protocols were approved by the University of North Carolina (UNC) at Chapel Hill's Institutional Animal Care and Use Committee and were verified to follow guidelines from the National Institutes of Health concerning use of vertebrate animals in research.

Smoke inhalation. Mice were anesthetized using tribromoethanol (475 mg/kg; Sigma-Aldrich), and their dorsum was shaved (NC0854145; Fisher) before injection of subcutaneous morphine sulfate (3 mg/kg; Westward). Mice were then placed on an intubation platform (Penn Century). The trachea was visualized with a laryngoscope, and a cannula (22 G × 1 in.; Exel) was placed in the trachea. Mice were kept in a supine position and placed in an animal induction chamber (NC9296517; Stoelting). Plywood sectioned into strips (2.5 × 8 cm, allowed to equilibrate in a 45% humidity and 65°F temperature controlled room for 2 wk before the experiment, item no. 12206, model no. 776391100000; Lowe's) was placed in a side-arm flask on a heat block set to 500°C, causing the board to smolder and produce smoke (outlined in Fig. 1A). Wood (~50 g) was used at the start of experiments, with additional pieces added as needed. Air pumped through the flask forced smoke in the induction chamber for three exposures of 2 min with a 1-min break between exposures. Clear walls of the induction chamber allowed visual assessment of smoke density; air pressure was kept constant, and the chamber was vented or kept sealed to maintain smoke density that resulted in visual obstruction at 1–1.5 in. In a closed chamber under our prescribed exposure conditions, we quickly reached the maximum value of optical density attained by plywood smoke (295 for unfinished plywood; see Ref. 18). For the first preliminary experiments we used a photometer, and the smoke density exceeded the maximum specific optical density and therefore the meter's range (18), and that density was the only density to produce significant particle accumulation in the lungs. We used a filter placed in the circuit that allowed us to weigh the deposited smoke particles, which we found to be consistent between experiments. The time taken to reach the maximum specific optical density was also consistent between experiments. Moreover, visual inspection of catheters removed from mouse airways confirmed deposition of soot on the end of the catheters (Fig. 1B) and upper airways; soot was similarly observed in the trachea of mice euthanized within 24 h of inhalational injury (Fig. 1C). The heat plate, flask, and induction chamber were set up in a dedicated fume hood as outlined in Fig. 1A. Mice were allowed to recover on a heating pad, were resuscitated with an intraperitoneal injection of lactated Ringer's solution (1 ml/kg body wt; Baxter Healthcare), and were given morphine in their drinking water ad libitum for the duration of the experiment. Sham mice were treated identically except that air was pumped in the induction chamber rather than smoke. Before tissue collection, mice were euthanized with gaseous isofluorane.

Bacterial infection. Pseudomonas aeruginosa (strain PA01) was grown in Luria-Bertani (LB) broth at 37°C with shaking to reach the midlog phase growth. Bacterial pellets were washed and resuspended with cold PBS with 1% Protease Peptone (PP-PBS) and diluted to 5×10^6 colony-forming units (CFU)/ml. Serial dilutions of inoculum were plated on LB agar to confirm bacterial dosage. Inoculum (200 μl) was administered to mice via tail vein injection; mock-infected mice received 200 μl PP-PBS. Bacterial burden in the airway at time of harvest was determined by plating 100 μl of BALF in duplicate on LB agar. Bacterial burdens in liver and spleen were determined by plating serial dilutions of organ homogenate in PP-PBS on LB agar plates.

Fig. 1. Development of an animal model of inhalation injury. Schematic of the laboratory setup of the smoke inhalational model (*A*), deposition of soot on the cannula used to intubate the mice undergoing injury (*B*), and smoke particles within lung lobes of injured mice (*C*).
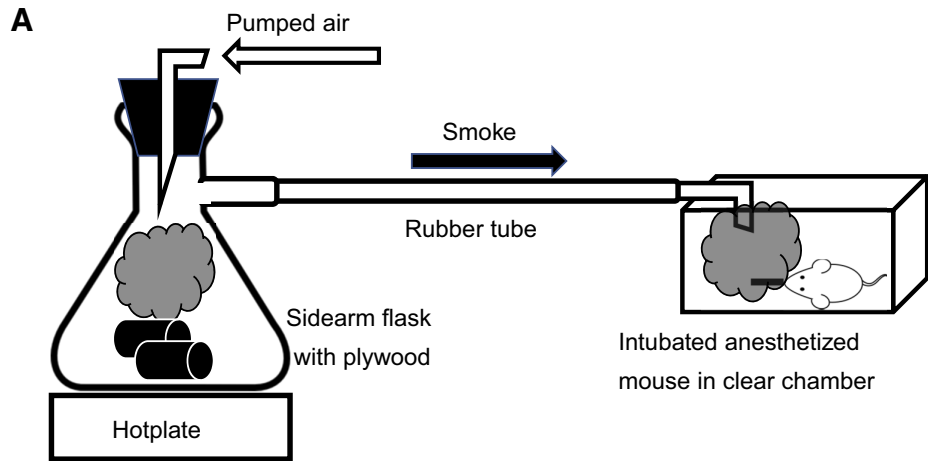
Bronchoalveolar lavage sample acquisition and processing. To collect BALF, a catheter (22 G × 1 in.; Exel) was inserted in the trachea and connected to a syringe containing 1 ml 0.6 mM EDTA in PBS; 0.6 ml was instilled in the lungs and then withdrawn three times to obtain a primary wash. Typical recovery was 0.75 ml. Two subsequent washes were combined to obtain a secondary wash, for which typical recovery was 2 ml. Cell pellets from primary and secondary washes were combined for analysis via flow cytometry or pelleted and stored at −80°C for subsequent analysis by qPCR.

Cell-free supernatant from primary wash was analyzed by Bradford assay and enzyme-linked immunosorbent assay for IL-10, hyaluronic acid, CXCL1, CXCL2 (R&D), IL-12, and MCP-1 (eBioscience) according to the manufacturer's instructions. Cell-free DNA was enriched from secondary BALF supernatant. Briefly, 500 μl of BALF supernatant were treated with 50 μl of Proteinase K solution and 125 μl of S&P Proteinase K Digestion Buffer (Zymo Research, Irvine, CA). Following proteinase K addition, samples were incubated for 30 min at 55°C and then 2.7 volumes of S&P DNA binding buffer (Zymo Research) were added to each sample. Samples were then mixed and added to Zymo-Spin III-S columns for DNA isolation per the manufacturer's protocol. Cell-free dsDNA (cfDNA) was eluted from the column using 50 μl of prewarmed DNA Elution Buffer (Zymo Research). Total cfDNA per millilter of BALF input was determined using the Qubit 3.0 fluorimeter (Life Technologies) and the Qubit dsDNA high-sensitivity detection reagents (Life Technologies).

Lungs were removed from mice after lavage. Minced lung tissue was digested in 4 ml PBS with 10% fetal bovine serum (PBS-FBS), 1,500 μg/mouse collagenase (Worthington), and 0.1 μg/mouse DNase and shaken at 250 rpm at 37°C for 1 h. Samples were filtered through a 100-μm cell strainer. Red blood cells were removed with ACK Lysis Buffer, and remaining cells were suspended in PBS-FBS before flow cytometric analysis. Live cells from lung digest and BALF were counted manually with a hemocytometer using 0.01% trypan blue cell viability dye (Life Technologies).

Flow cytometry. Following incubation with Fc Block (eBiosciences), cells were stained with labeled antibodies against CD45, CD11b, CD11c, and Ly6G (eBiosciences; BD Biosciences). Cells were fixed with 1% paraformaldehyde before analysis on a CyAn (Beckmann-Coulter). Samples were analyzed with Summit 5.1 software (Beckmann-Coulter). Following exclusion of CD45-CD11b-CD11c$^-$ cells, Neutrophils were defined as CD45$^+$CD11b$^+$CD11c$^-$Ly6G$^+$, and macrophages were defined as CD45$^+$CD11c$^+$Ly6G$^-$.

Isolation and analysis of gene expression by qRT-PCR. Total RNA was isolated using the RNeasy Mini-RNA extraction kit (Qiagen) for BALF cells and the RNeasy Mini-RNA Fibrous Tissue kit (Qiagen) from mouse whole lungs. Reverse transcription reactions were performed with the VILO Reverse Transcription master mix (Life Technologies) using 0.25 μg of total RNA. Real-time qRT-PCR was performed using the QuantStudio 6 (Life Technologies) machine and TaqMan Gene Expression master mix (Thermo-Fischer). Each reaction contained 1× TaqMan Gene Expression master mix, cDNA from 40 ng of RNA, and 1× of gene-specific primer/probe combinations (catalog no. 4331182; Gapdh Primer ID Mm99999915_g1, TATA box-binding protein Primer ID Mm01277042_m1, IL-10 Primer ID Mm01288386_m1, NOS2 Primer ID Mm 010927.3, IL-12b Primer ID Mm01288989_m1, matrix metalloproteinase (MMP)-8 Primer ID Mm00439509_m1, MMP9 Primer ID Mm00442991_m1; Life Technologies) in a total volume of 20 μl. PCR was performed in duplicate by cycling at 50°C for 2 min and 95°C for 15 min followed by 40 cycles of denaturation at 95°C for 10 s and annealing and extension at 60°C for 30 s. Values were derived using the $\Delta\Delta C_T$ method comparing sham mice with inhalation injury mice at each time point, and mRNA levels were normalized to housekeeping genes (GAPDH and TATA box-binding protein).

Isolation and analysis of cytokine and chemokine levels by multiplex analysis. BALF was collected as above, and we employed multiplex analysis of 33 chemokines and cytokines (BCA-1/CXCL13, CTACK/CCL27, ENA-78/CXCL5, Eotaxin/CCL11, Eotaxin-2/CCL24, Fractalkine/CX3CL1, GM-CSF, I-309/CCL1, interferon-γ, IL-1β, IL-2, IL-4, IL-6, IL-10, IL-16, IP-10/CXCL10, I-TAC/CXCL11, KC/CXCL1, MCP-1/CCL2, MCP-3/CCL7, MCP-5/

CCL12, MDC/CCL22, macrophage inflammatory protein (MIP)-1α/CCL3, MIP-1β/CCL4, MIP-2/CXCL2, MIP-3α/CCL20, regulated upon activation normal T cell expressed and secreted/CCL5, MIP-3β/CCL19, SCYB16/CXCL16, stromal cell-derived factor-1α/CXCL12, TARC/CCL17, TECK/CCL25, tumor necrosis factor-α) according to the manufacturer's instructions (Bio-Plex Pro Mouse Chemokine Panel 33-Plex no. 12002231; Bio-Rad).

Histopathology. To prepare lung tissue for histology, lungs were inflated with 4% paraformaldehyde in PBS to a constant pressure of 20 cmH$_2$O. Inflated tissue was stored overnight in 4% paraformaldehyde and then rinsed with 70% ethanol. Left lobes were embedded in paraffin, and 4-μm sections of tissue containing large airway branches were cut and stained with hematoxylin and eosin at the UNC Chapel Hill Animal Histopathology Core Facility. Images of deidentified specimens were taken at the UNC Microscopy Services Laboratory using an Olympus BX61 light microscope. At least 10 nonoverlapping images of distal lung tissue (excluding major blood vessels and large airways) were taken per specimen using the UPlanFLN 40×/0.75 objective. The UPlanFLN 20×/0.50 objective was used to obtain sequential images of a large airway. Images of the distal lung tissue were scored on a scale of 0 (normal) to 2 (maximal) for neutrophil infiltration, proteinaceous debris, and congestion in microvasculature. Images of large airway sections were scored for the same traits in addition to cytoplasmic vacuolization and soughing of airway epithelial cells. For each characteristic, the average score for 10–15 images/specimen was calculated, and the sum of those values was obtained to produce a cumulative tissue damage score (Table 1). Reported scores were obtained by a single blinded individual, and findings were confirmed by a second blinded individual.

Patient Samples. Patient BALF was obtained and analyzed as previously described (22). Briefly, subjects were admitted to the North Carolina Jaycee Burn Center at UNC who carried diagnoses of inhalation injury and were intubated with mechanical ventilation. Subjects were enrolled over a 2-yr period and followed until discharge or death. Serial bronchial washings from clinically indicated bronchoscopies were collected and analyzed for markers of tissue injury and inflammation. This study was approved by the UNC Biomedical Institutional Review Board (study no. 10–0959). In this analysis we excluded subjects for whom HA was only measured at *days 0* and *1*.

Statistical analysis. GraphPad Prism version 5.0 for Windows was used to analyze data by Student's *t*-test, one-way analysis of variance (ANOVA) with Tukey's posttest, or two-way ANOVA with Bonferroni posttest, as appropriate. In cases where data are represented in relation to sham average, one-sample *t*-test was used to compare values and means with a hypothetical value of 1. Data are presented as means ± SE. Statistical significance is indicated at the 0.05, 0.005, and 0.001 levels.

Table 1. *Histopathological scores of DLT and LA at 24 and 96 h after smoke inhalation or sham procedure*

	Sham	24 h	96 h
DLT			
Neutrophils	0.16 (0.10)	0.42 (0.22)	0.57 (0.29)
Proteinaceous debris	0.42 (0.12)	0.64 (0.40)	0.36 (0.04)
Congestion	0.06 (0.05)	0.21 (0.23)	0.45 (0.29)
Cumulative DLT score	0.64 (0.14)	1.27 (0.76)	1.38 (0.37)*
LA			
Neutrophils	0.00 (0.00)	0.00 (0.00)	0.04 (0.08)
Sloughing	0.07 (0.06)	0.01 (0.03)	0.04 (0.05)
Cytoplasmic blebbing	0.45 (0.22)	0.39 (0.22)	0.25 (0.17)
Cytoplasmic vacuolization	0.05 (0.09)	0.84 (0.16)**	0.09 (0.15)
Congestion	0.06 (0.07)	0.12 (0.20)	0.13 (0.11)
Cumulative LA score	0.63 (0.16)	1.37 (0.58)*	0.56 (0.43)

Values are means (SD); *n* = 4 mice/treatment group, pooled from 2 separate experiments. DLT, distal lung tissue; LA, large airway. *$P < 0.05$ and **$P < 0.005$.

RESULTS

Inflammatory cells migrate to the lung after smoke inhalation. BALF from sham mice and mice who were exposed to plywood smoke was used to enumerate live cells and analyze the total protein content in BALF supernatants. Quantification of live cells in the BALF revealed increased cell numbers at 24, 48, 72, and 96 h following smoke inhalation compared with sham-treated controls (Fig. 2A). There was also an increase in the total protein concentration in BALF from smoke-exposed mice at 24 and 96 h postinjury (Fig. 2B). Using flow cytometry to characterize cells isolated from the BALF, we observed an increase in the total number of neutrophils following smoke inhalation compared with sham-treated mice (Fig. 2C). In contrast, macrophage numbers in the BALF were not significantly altered by smoke inhalation (Fig. 2D). Lung digests revealed that smoke inhalation did not cause a significant change in the number of either neutrophils or macrophages in interstitial lung tissue at 24, 48, or 96 h (Fig. 2, E and F). Although there are sex differences in patient and murine responses to burn (36) that lead to a suppression of inflammation, we observed a similar influx of neutrophils and macrophages to the airway of male mice compared with females (Fig. 2, C and D). We therefore used female mice for the rest of the study to be consistent with previous studies using our murine cutaneous burn models (5–7, 14, 28, 34).

To characterize polarization of immune cells in the BALF, expression of *Nos2* mRNA was quantified by qRT-PCR. *Nos2* mRNA was significantly increased in immune cells isolated from smoke-treated mice relative to sham-treated mice at 24 and 48 h postinjury (Fig. 2G). RNA expression of MMP8 (also known as neutrophil collagenase) and MMP9 (gelatinase B) was also quantified in cells extracted from BALF by qRT-PCR. We observed an increase in the expression of MMP9 but not MMP8 at both 24 and 96 h following smoke inhalation compared with sham-treated mice (Fig. 2H). By contrast, smoke inhalation did not cause a change in either MMP8 or MMP9 in interstitial lung tissue (data not shown).

To characterize damage to lung tissue following smoke inhalation, sections of fixed lung tissue were analyzed for five indicators of histopathology, and a tissue damage score was calculated for both distal lung tissue and large airway epithelium (Table 1). Quantitative assessment of lung damage by blinded observers indicated significant damage to the large airways at 24 h and to distal lung tissue at 96 h postsmoke inhalation (Fig. 3, A and B). Proteinaceous and cellular congestive material was seen within the alveolar spaces of smoke-treated mice compared with sham-treated mice, consistent with the greater concentration of protein observed in the BALF (Fig. 3, D and E). Analysis of specimens taken 96 h following smoke inhalation indicated greater congestion of the pulmonary microvasculature and mild thickening of the alveolar walls due to both congestion and edema in distal lung tissue (Fig. 2E). We observed cytoplasmic vacuolization and sloughing in epithelial cells of the large airways of smoke mice compared with sham within 24 h of smoke inhalation (Fig. 3, F and G) as well as debris and occasional aggregates of macrophages at 96 h (Fig. 3H).

IL-10 expression precedes HA DAMP release following smoke inhalation. We have previously demonstrated that elevated IL-10, a skewed IL-10-to-IL-12 ratio, and elevations in
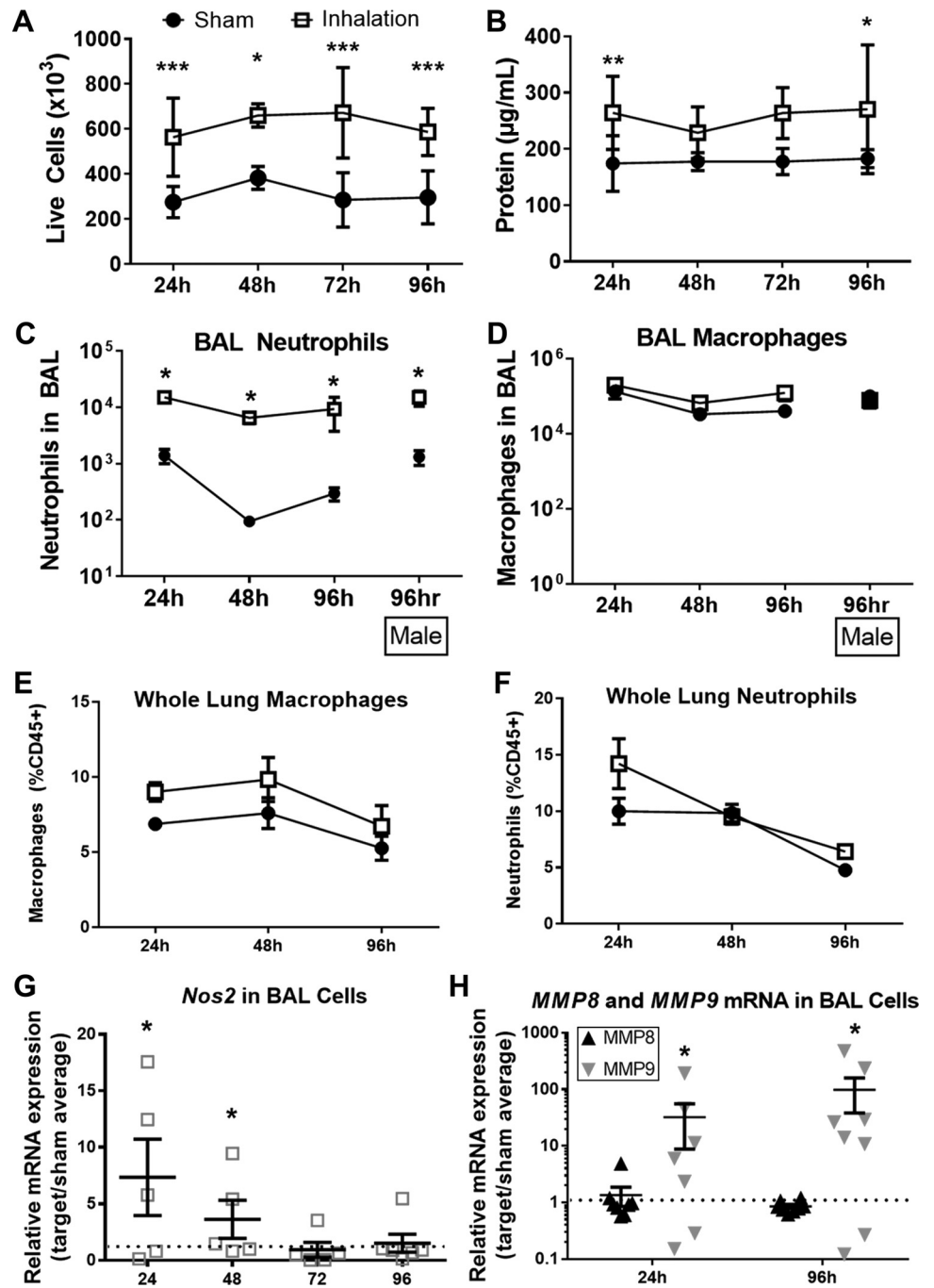
Fig. 2. Neutrophilic inflammation following acute wood smoke inhalation. *A*: total live cells were enumerated in bronchoalveolar lavage fluid (BALF) at indicated time points following smoke or sham procedure. *B*: protein concentration in BALF cell-free supernatant was measured by Bradford assay. *C–F*: neutrophils and macrophages were quantified by flow cytometry and normalized to live cell counts in BALF (*C* and *D*) and whole lung (*E* and *F*) following injury. *G* and *H*: *Nos2* (*G*) and matrix metalloproteinase (MMP)-8 and MMP9 (*H*) mRNA expression was measured in BALF cells at indicated time points after smoke procedure and were normalized to sham average at each time point. Two-way ANOVA with Tukey's posttest (*A–F*) or 1-sample *t*-tests vs. sample value = 1 (*G* and *H*) were used to determine statistical significance at all time points. *$P <$ 0.05, **$P <$ 0.005, and ***$P <$ 0.001, representative of 3 repeated experiments. No. of mice as follows: $n = 5$ sham and $n = 6$ inhalation injury (*A–F*), 5 sham and 6 inhalation injury (*G*), and 5 sham and 7 inhalation injury (*H*) mice.

the DAMPS dsDNA and HA are reliable predictors of patient outcomes following inhalation injury although the mechanistic relationship between these biomarkers and subsequent infection has not yet been established (22, 29). In mice exposed to plywood smoke, IL-10 was significantly elevated in BALF at 24 h compared with uninjured mice; however, the increase was transient and was not significant at subsequent time points (Fig. 4*A*). These data are supported by qRT-PCR, which illustrated an increase in IL-10 mRNA in cells recovered from the BALF of injured animals normalized to sham average at 24 h (Fig. 4*B*), normalizing relative to sham-treated mice between 48 and 96 h. No significant changes in IL-12 protein or mRNA in BALF were observed at any time (data not shown). In

lung tissue, no statistically significant changes in IL-10 gene expression were observed at either 24 or 96 h (Fig. 4*C*). IL-12 gene expression was significantly downregulated in lung tissue at 96 h following smoke inhalation compared with controls (Fig. 4*C*).

To establish the presence of DAMPs in the animal model, which have been used to predict patient outcome, HA and cfDNA were measured in BALF following smoke inhalation or sham procedure. The sham procedure did not change levels of HA or dsDNA at any time point evaluated (Fig. 4, *D* and *E*). By contrast, cfDNA was elevated in injured mice compared with shams at 12–24 h before returning to baseline by 48 h (Fig. 4*D*). In addition, we observed that concentrations of HA
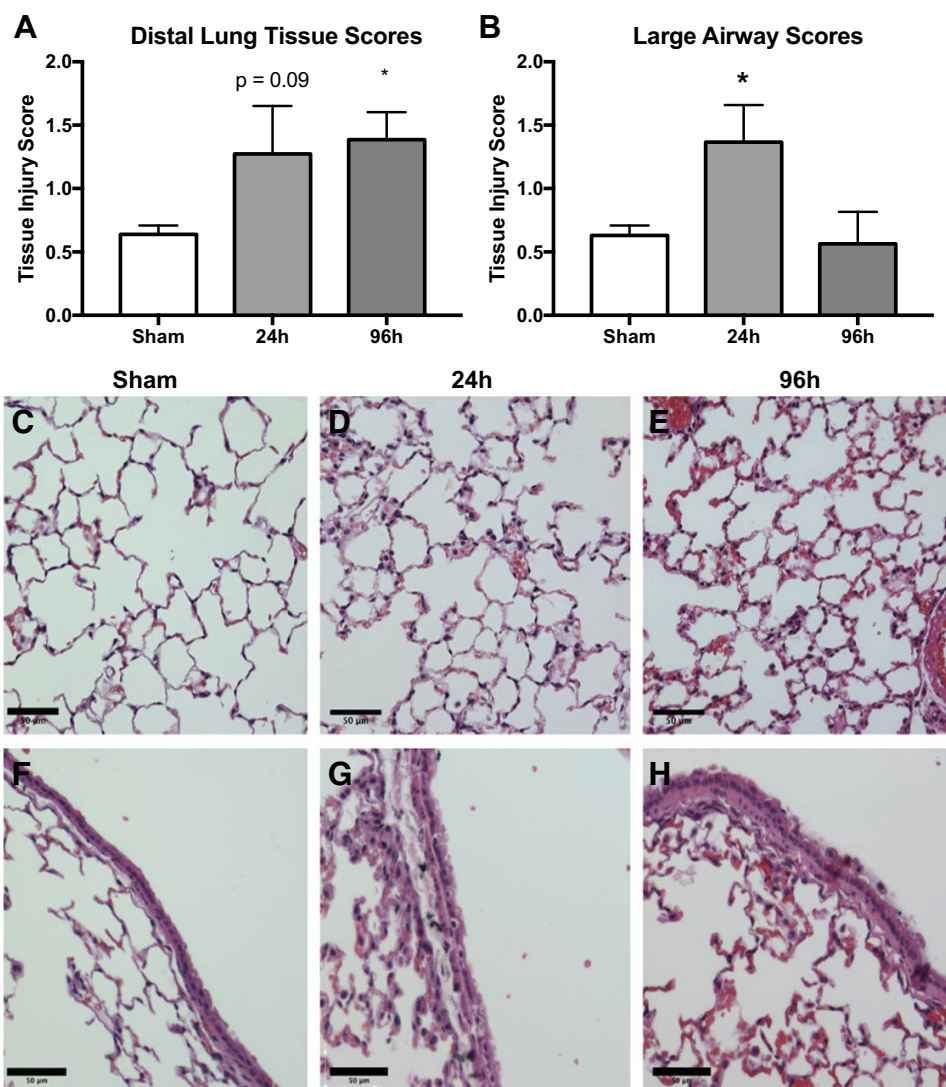
Fig. 3. Histological evidence of lung injury following acute smoke exposure. Sections of lung tissue were analyzed by histology and scored by blinded individuals. Tissue injury score in sections of distal lung tissue sections (*A*) and large airway sections (*B*) in pooled sham mice and smoke-treated mice at 2 time points. *P* value represents Tukey's posttest following a 1-way ANOVA. Representative images of distal lung tissue from sham (*C*), 24-h post-smoke-treated (*D*), and 96 h post-smoke-treated (*E*) mice are shown. Representative images of large airway from sham (*F*), 24 post-smoke-treated (*G*), and 96-h post-smoke-treated (*H*) mice are shown. Scale bars correspond to 50 μm. *$P < 0.05$ and ***$P < 0.001$, representative of 3 experiments; $n = 5$ sham and 6 inhalation injury mice (*A* and *B*).
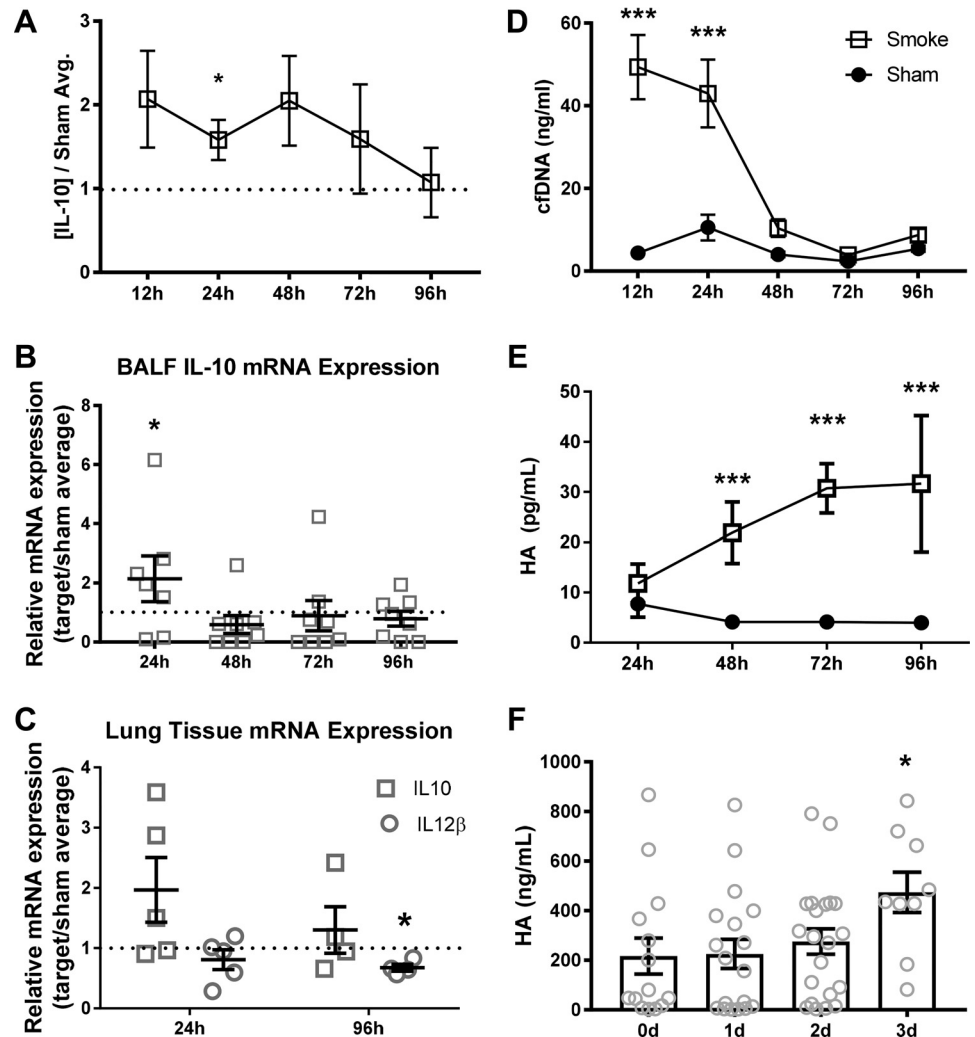
increased over time following smoke inhalation, reaching a peak at 72–96 h (Fig. 4*E*). We analyzed our patient data and found that this late peak in BALF HA expression in the mouse model of inhalational injury was mirrored in patients diagnosed with inhalational injury (Fig. 4*F*).

Pulmonary infection develops after systemic inoculation in mice following smoke inhalation. Patients diagnosed with inhalational injury frequently develop pneumonia following colonization by opportunistic bacteria, most commonly *P. aeruginosa* (6). We therefore propose that any clinically relevant animal model of smoke inhalation injury should render mice susceptible to bacterial challenge that does not cause infection in uninjured mice. Mice were exposed to an intravenous inoculation with *P. aeruginosa* (strain PA01) 48 h following smoke exposure or sham treatment. The recovery of bacteria from BALF was quantified at 24, 48, and 96 h following infection (Fig. 5*A*). In sham mice we detected nominal, if any, bacteria in the BALF; after smoke inhalation, we consistently observed substantial CFUs from BALF significant amounts of bacteria at 24, 48, and 96 h after inoculation. Bacterial recovery from the systemic compartments of the liver and spleen tissue was sporadic and unaltered by injury status (data not

shown). Infection further exacerbated pulmonary damage in the smoke-injured mice, demonstrated by increased concentrations of protein and HA in the BALF compared with sham mice (Fig. 5, *B* and *C*). Taken together, these data demonstrate using bacterial infection as a clinically relevant readout; these data demonstrate that we have developed a model of woodsmoke inhalation that closely recapitulates the immunosuppressive sequalae seen in humans.

Differential regulation of injury phenotypes by Nos2. Nos2 activity is known to modulate neutrophil recruitment and activation as well as cytokine and chemokine production (3). Nos2 expression has been demonstrated to be increased following smoke inhalation (33, 39). We therefore designed a series of experiments to determine the impact of Nos2 expression on inflammation following acute smoke inhalation. Nitric oxide synthase-deficient ($Nos2^{-/-}$) mice were either subjected to wood smoke inhalation injury or sham procedure, after which BALF and susceptibility to infection were evaluated as previously described. Neither BALF protein nor neutrophil accumulation after smoke inhalation was different in $Nos2^{-/-}$ mice compared with wild-type controls at either 24 (data not shown) or 96 (Fig. 6, *A* and *B*) h. Similarly, whereas IL-10 and

Fig. 4. IL-10 precedes damage-associated molecular pattern (DAMP) release following smoke inhalation. *A*: IL-10 concentration in primary BALF cell-free supernatant following inhalational injury, normalized to sham average concentrations at each time point. *B*: IL-10 mRNA expression in BALF cells normalized to sham average at indicated time points after injury. *C*: IL-10 and IL-12 mRNA expression in lung tissue, normalized to sham average expression at each time. *P* values reflect 1-sample *t*-tests vs. sample value = 1. *D* and *E*: cell-free double-stranded DNA (cfDNA) concentration in secondary BALF supernatant (*D*) and hyaluronic acid concentration in primary BALF supernatant (*E*) were analyzed by 2-way ANOVA with Tukey's posttest to determine significance between groups at each time point. *F*: hyaluronic acid concentration in BALF samples from patients diagnosed with inhalational injury, and *P* value represents 1-way ANOVA with posttest vs. *day 0* (0d) concentrations. *$P < 0.05$ and ***$P < 0.001$, representative of 3 experiments. No. of mice as follows: $n = 5$ sham and 6 inhalation injury (*A*, *D*, and *E*), 5 sham and 8 inhalation injury (*B*), 5 sham and 5 inhalation injury (*C*), and 5 sham and 10 (0d), 15 (1d), 24 (2d), and 12 (3d) inhalation injury (*F*) mice.

MCP-1 were elevated in BALF 24 h following smoke inhalation in wild-type mice, a similar increase was absent in $Nos2^{-/-}$ mice (Fig. 6, *C* and *D*). In addition, the inhalation injury-induced increase in BALF HA concentration at 96 h was also attenuated in $Nos2^{-/-}$ mice, and we did not observe a significant increase in BALF dsDNA concentrations at 24 h after inhalational injury in $Nos2^{-/-}$ mice (Fig. 6, *E* and *F*). Finally, a Nos2-dependent difference in bacterial clearance
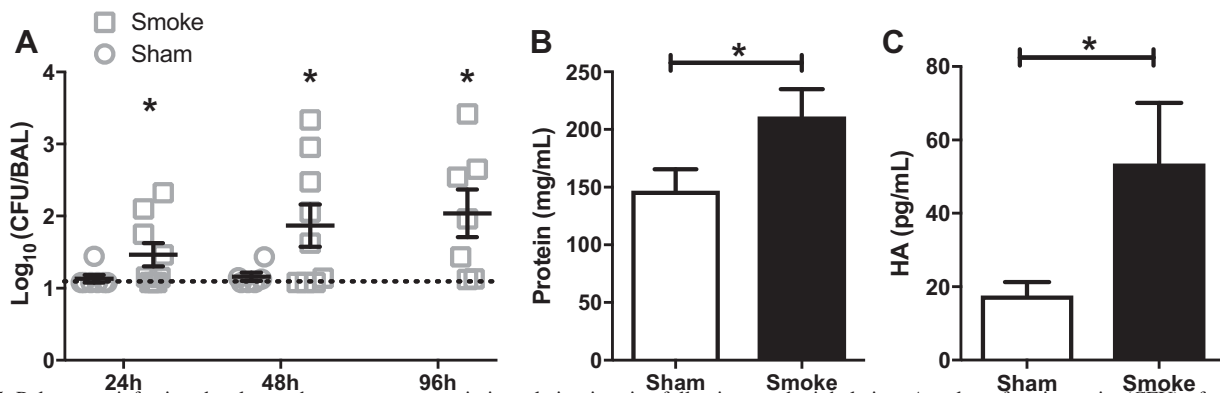

Fig. 5. Pulmonary infection develops subsequent to systemic inoculation in mice following smoke inhalation. *A*: colony-forming units (CFU) of recovery from BALF of mice infected with 1×10^6 CFU PA01 at 48 h after sham or smoke procedure and harvested at various time points following infection. Broken line represents the limit of detection. *B* and *C*: protein concentration (*B*) and hyaluronic acid (*C*) concentration in BALF cell-free supernatant of mice infected with 1×10^6 CFU PA01 at 48 h after sham or smoke procedure and harvested 48 h after infection; data are pooled from 3 independent experiments. *P 0.05. No. of mice as follows: n 6 sham and 9 (24 h), 10 (48 h), and 7 (96 h) inhalation injury (*A*) and 5 sham and 5 inhalation injury (*B* and *C*) mice.
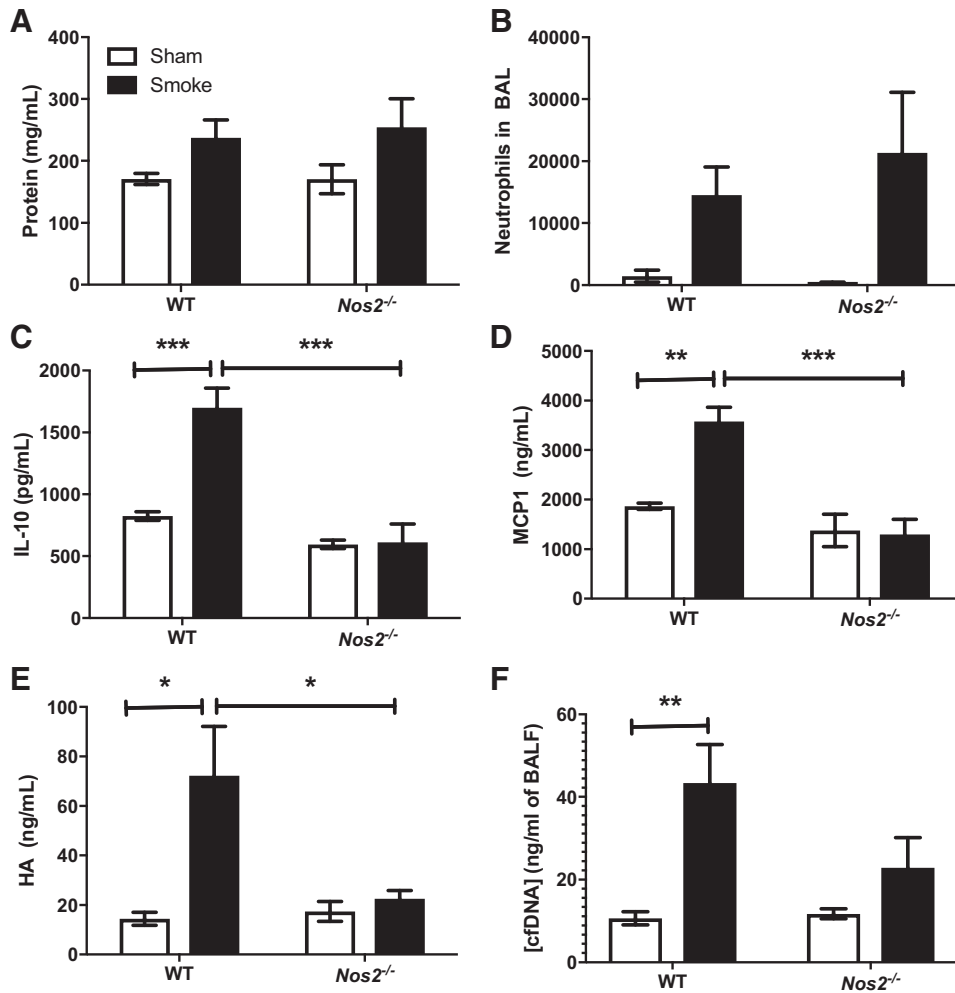
Fig. 6. Nos2 deficiency reverses IL-10, monocyte chemoattractant protein (MCP)-1, and hyaluronic acid (HA) after smoke inhalation. *A*: protein concentration in BALF at 96 h following sham or injury procedure. *B*: neutrophils quantified by flow cytometry and normalized to live cell counts in BALF at 96 h following injury. *C* and *D*: IL-10 (*C*) and MCP-1 (*D*) concentration in BALF at 24 h. *E*: HA concentration in BALF at 96 h. *F*: cfDNA concentration in BALF at 24 h. Data are pooled from 3 independent experiments. Data were analyzed by 2-way ANOVA with Tukey's posttest. *$P < 0.05$, **$P < 0.005$, and ***$P < 0.001$. No. of mice as follows: $n = 5$ sham and 6 inhalation injury mice.

following an intravenous challenge of *P. aeruginosa* was not observed (data not shown).

CXCL1 drives lung neutrophil accumulation and infection clearance in the lung following smoke exposure. To delineate potential chemotactic signals responsible for neutrophil recruitment to the airway following smoke inhalation, we measured the neutrophil chemoattractants CXCL1 (also known as KC) and CXCL2 (also known as Gro2 and Mip2) in BALF. At 24 h postinjury we observed an increase in CXCL1 in BALF; however, CXCL1 concentrations returned to baseline at all subsequent time points (Fig. 7*A*). We did not detect CXCL2 in injured mice at any time following injury (data not shown).

To determine whether CXCL1 was responsible for neutrophil recruitment to the airway following inhalational injury, a CXCL1-neutralizing antibody (or isotype control) was administered intravenously at 0.5 and 24 h after smoke exposure. Treatment with anti-CXCL1 resulted in a decrease in total BALF neutrophil numbers at 48 (8.9-fold, $P = 0.03$) and 72 (3.3-fold, $P = 0.01$) h compared with smoke-exposed mice treated with an isotype control (Fig. 7*B*). To determine whether complete inhibition of neutrophil trafficking could be achieved with higher antibody concentration, a series of increased concentrations of neutralizing antibody was used. Increased concentrations of neutralizing antibody did not further decrease neutrophil numbers (data not shown), which suggests that

additional chemotactic signals contribute to neutrophil recruitment, or can partially compensate for CXCL1.

To test whether attenuated neutrophil recruitment following tissue injury impacted subsequent sensitivity to bacterial lung infection, we intravenously infected anti-CXCL1 and isotype-treated mice 48 h following inhalation injury with 1×10^6 CFU PA01 (experimental schematic in Fig. 7*C*). Pulmonary bacterial burden was quantified 2 days after infection by CFU analysis of BAL (Fig. 7*D*). Significantly less bacteria were recovered from the airway of mice treated with anti-CXCL1 compared with those treated with isotype control (Fig. 7*D*). Recruitment of neutrophils to the airway (Fig. 7*E*), protein accumulation within the BALF (Fig. 7*F*), and HA accumulation (Fig. 7*G*; modest yet significant decrease of ~10%, which is unlikely to have biological significance) were unaltered by administration of anti-CXCL1.

CXCL1 drives lung damage, inflammatory cytokine, and chemokine following smoke exposure. Anti-CXCL1 antibody reduced accumulation of neutrophils after smoke exposure (Fig. 7*B*) yet did not impact subsequent neutrophil recruitment following bacterial infection (Fig. 7*E*) and promoted increased clearance of bacterial burden (Fig. 7*D*). Therefore, to examine the possible mechanism(s) of the increased bacterial clearance, we quantified the histopathology at 24 h after inhalation injury (in the absence of infection) in mice treated with neutralizing

Fig. 7. CXCL1 drives lung neutrophilia and bacterial clearance following smoke exposure. *A*: CXCL1 concentration in BALF at 24–96 h. *B*: mice were treated with anti-CXCL1 or isotype control at 0 and 24 h following injury. Neutrophils were quantified by flow cytometry and normalized to live cell counts in BALF at 24 and 48 h following injury. *C*: experimental design. Mice were treated with anti-CXCL1 or isotype control antibody via tail vein injection at 0 and 24 h following smoke exposure. At 48 h mice were inoculated with PA01 or vehicle control via tail vein injection. Samples were collected at 48 h following infection, 96 h following injury. *D*: CFU recovery from BALF of smoke-treated mice treated with anti-CXCL1 or isotype control before infection with PA01. *E* and *F*: neutrophils from BALF quantified by flow cytometry (*E*) and protein concentration in BALF of infected mice treated with anti-CXCL1 or isotype control (*F*). *G*: HA concentration in BALF following smoke and infection in mice treated with anti-CXCL1 or isotype control. Data were analyzed by 2-way ANOVA with Tukey's posttest. *$P < 0.05$, ***$P < 0.001$ representative of 3 experiments. No. of mice as follows: $n = 5$ isotype and 6 anti-CXCL1 (*A* and *B*), 12 isotype and 9 anti-CXCL1 (*D*), and 5 isotype and 6 anti-CXCL1 (*E–G*) mice.
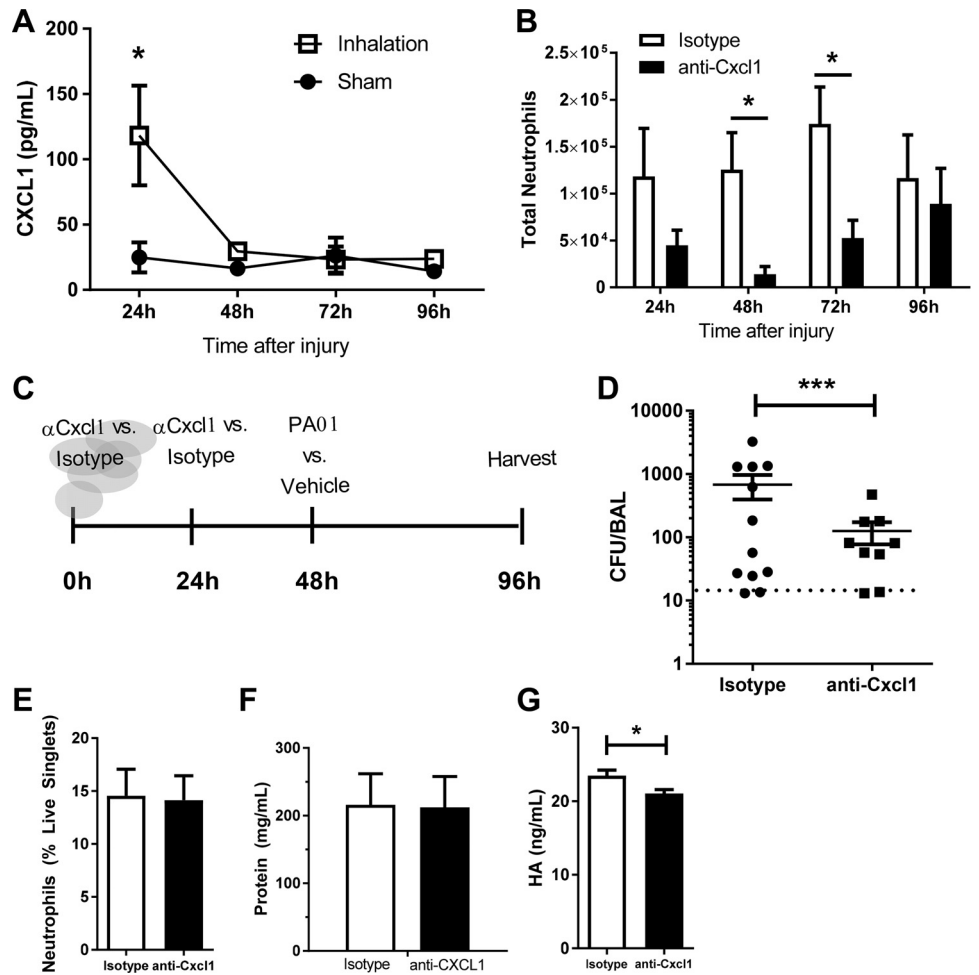
antibody or isotype control. We observed a significant decrease in tissue damage scores in distal airway specimens from mice treated with neutralizing antibody (Fig. 8*A*). This decrease was primarily attributable to a decrease in cellularity and debris congestion scores (0.93 ± 0.11 vs. 0.27 ± 0.28; $P < 0.05$); we did not observe any difference in protein levels released in the BAL (Fig. 8*B*).

We also characterized the effect of anti-CXCL1 treatment on the expression of an array of inflammatory cytokines and chemokines in the BALF early after injury (Fig. 8, *C–E*). We found that a subset of cytokines (IL-6, IL-1β, and IL-16; Fig. 8*C*) was significantly increased after injury compared with sham but significantly decreased at 24 h postinhalation injury by anti-CXCL1 treatment compared with injured animals treated with isotype-antibody. Reduction of these proinflammatory mediators may reflect reduction in neutrophils numbers and associated lung damage. In contrast, CXCL5 (ENA78) was significantly decreased by inhalation injury compared with sham but not significantly impacted by anti-CXCL1 antibody (Fig. 8*D*). A further subset of mediators (CCL25 and CXCL13; Fig. 8*E*) was significantly elevated 48–72 h after injury in anti-CXCL1-treated mice compared with isotype-treated animals. We hypothesize that these mediators are responsible for increased chemotaxis that aids bacterial clearance during infection.

DISCUSSION

Acute smoke inhalation and injury present a significant clinical challenge for inhabitants of regions at risk for wildfires, survivors of structural fires, first responders, and members of the armed forces. Inhalational injury is among a spectrum of stimuli that can precipitate acute lung injury (ALI) and acute respiratory distress syndrome (ARDS). Despite significant research into targeted therapies for ALI/ARDS, an effective pharmaceutical intervention does not currently exist (21). The initiation and outcome of inhalational injury and ALI are idiosyncratic, brought on by a multitude of stimuli, and result in outcomes impacted by a host of comorbidities, including inflammatory disorders and smoker status (21, 27, 31, 38). It is therefore critical that research into inhalational injury and ALI accounts for these complexities. Thus, preclinical animal models and studies should be designed to replicate, as faithfully as possible, the etiology of human disease.

Here we report the development and utilization of a murine model of acute exposure to smoke derived from plywood, a common building material. This model recapitulates many of the histopathological and immune phenotypes previously reported to predict outcomes in patients, including a predominance of neutrophils in the airway, expression of IL-10, and elevated DAMPs such as dsDNA and HA in the BALF fol-
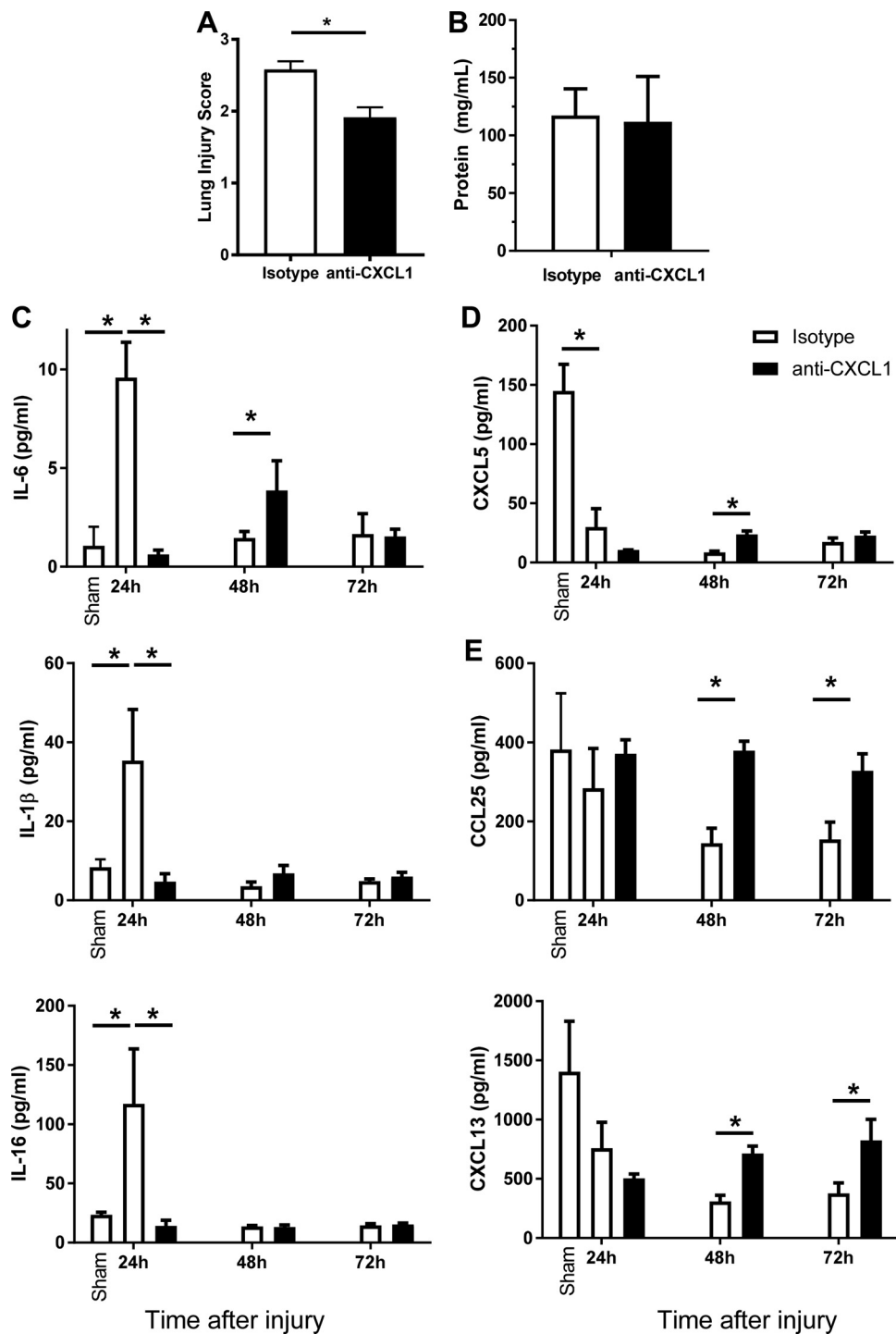
Fig. 8. Early inhibition of neutrophil migration protects against injury and induces specific chemokine and cytokine alterations. Mice were treated with anti-CXCL1 or isotype control antibody via tail vein injection at 0 and 24 h following smoke exposure. BALF samples were collected at 24, 48, and 72 h following injury. A: representative tissue injury scores from distal airway sections. B: protein concentration in BALF cell-free supernatant was measured by Bradford assay. C–E: multiplex analysis was performed on BALF samples from sham and injured animals with isotype or anti-CXCL1 antibody. Data were analyzed by 2-way ANOVA with Tukey's posttest. *$P < 0.05$, representative of 3 experiments. No. of mice as follows: $n = 5$ isotype and 6 anti-CXCL1 mice (A–E).

lowing injury (12, 22, 29). Experiments using hickory wood chips (untreated/seasoned) resulted in similar changes in protein concentration and cell numbers. Further studies will address the extent to which inflammation and tissue damage differ depending on the source of smoke. Based on studies using clinical samples, prevailing wisdom is that tissue damage following inhalation injury leads to DAMP release, and subsequent detection of DAMPs through scavenger receptors and other pattern recognition receptors triggers an anti-inflammatory signaling cascade to limit further damage resulting from

immunopathology. It is plausible that this evolutionary response may be intended to minimize inflammation that would compromise gas exchange across the alveolar-capillary barrier. These informative clinical studies are limited because of the challenges inherent in clinical research regarding the timing and frequency of sample acquisition, which is especially unique to this patient population. Data from the model presented here echo this published clinical data, suggesting that anti-inflammatory cytokine production occurs rapidly in the lung following injury. Clinical studies have also reported that

macrophage numbers in the airway do not change between the acute phase of ARDS and resolution; however, neutrophil numbers are subject to change based on disease state (12). We observed a similar phenotype in our model of acute exposure to plywood smoke. Specifically, we demonstrated that macrophage numbers in BALF are unaltered by the injury, whereas the number of neutrophils increases following smoke inhalation (Fig. 1, C–F). The model also suggests a more delayed mechanism of tissue damage typified by delayed HA release (Fig. 4, E and F), which will be the focus of later investigation. Therefore, this model can and will be used to further clarify the dynamic relationship between DAMPs release and induction of anti-inflammatory processes within the injured lung.

Because pneumonia poses a significant comorbidity and challenge to patient recovery, any faithful animal model must recapitulate susceptibility to opportunistic infection. In our model of smoke inhalation, mice exposed to smoke from plywood are susceptible to pulmonary infection following a systemic bacterial challenge. Isolated smoke inhalation (as opposed to burns) likely predisposes patients to more tracheobronchial colonization with pathogen from an airborne route of exposure, as opposed to bacteremia-induced lung injury. Although our infection is restricted to the airway and is not detectable in the liver or the spleen, one bias of the model presented here is the route of infection leading to pulmonary bacterial colonization. While we have used a direct intratracheal aerosol route in previous studies (14, 32, 34), intratracheal infections cause inflammation in both injured and uninjured mice. In this study, we aimed to use an infectious challenge that would remain "subclinical" in uninjured mice; thus, we avoided direct intratracheal inoculation. In addition, even in the absence of cutaneous burn injury, patients with inhalational injuries require intravenous fluids, and catheter-related bloodstream infections are a significant cause of morbidity and mortality in burn units where bloodstream infections are thought to be a major source of the bacteria that colonize and establish active infections in other organs, including the lungs. Together these findings increase the translatability of this infection model.

Importantly, because of the challenges inherent in clinical research regarding the timing and frequency of sample acquisition, this model clarifies the dynamic relationship between DAMPs and anti-inflammatory cytokines in the injured lung. Prevailing wisdom is that tissue damage leads to DAMP release, and detection of DAMPs through scavenger receptors and other pattern recognition receptors triggers an anti-inflammatory signaling cascade to limit further damage resulting from immunopathology. Data from this model echo published clinical data suggesting that anti-inflammatory cytokine production occurs rapidly in the lung following injury; this evolutionary response may be intended to minimize inflammation that would compromise gas exchange across the alveolar-capillary barrier. The model also suggests a more delayed mechanism of tissue damage typified by delayed HA release, which will be the focus of later investigation.

We used this novel and clinically applicable model of inhalation injury to evaluate mechanisms that lead to the increased susceptibility of opportunistic infections. Specifically, we probed the contributions of Nos2 and IL-8 (CXCL1/ KC). Others have reported that, in mice, cotton smoke inhalation with and without burn injury led to an increase in Nos2 expression and activity in the airway (33) and that Nos2 is expressed in macrophages and airway epithelial cells following sepsis (8). In the current study we observed that, in the absence of Nos2, many relevant injury phenotypes are absent or significantly attenuated. Notably, Nos2 deficiency prevents smoke-induced elevation of IL-10 and MCP-1 at 24 h, as well as the release of HA but not cfDNA. These changes did not, however, impact neutrophil recruitment or damage to the alveolar-capillary barrier. Moreover, in support of other studies that have demonstrated that Nos2 expression and activity is dispensable for clearance of *P. aeruginosa* infection, we do not observe any change in bacterial clearance in injured mice deficient for Nos2 (4). It is worth noting that, in clinical studies, we have reported that BALF levels of both IL-10 and dsDNA correlate with the onset or susceptibility of infection (22, 29). This contrasts with our data that indicate that dsDNA can be elevated without a concomitant increase in IL-10 and that these changes do not alter the outcomes following bacterial challenge.

Significant clinical data suggest that expression of the potent neutrophil chemoattractant IL-8 is elevated following trauma and that its activity is a key determinant of clinical outcomes (10, 40). For instance, a spike in IL-8 is observed in patient serum following burn injury in the absence of sepsis (40), and, in a study of inhalational injury, IL-8 was elevated in survivors compared with those who succumbed to the injury (10). Conversely, in an animal model, inhibition of the murine IL-8 homolog CXCL1 (also known as KC) following burn resulted in a decrease of several markers of lung injury (43). Here we demonstrate that intravenous administration of a neutralizing antibody against CXCL1 attenuates but does not abolish neutrophil recruitment to the airway following inhalation injury. This phenotype corresponded with decreased tissue histopathology (Fig. 8B) and did render the mice less susceptible to infection (Fig. 7D). These data imply that neutrophils accumulate under the direction of CXCL1 (Fig. 7B) after woodsmoke and preinjure the lung, making bacterial clearance less efficient (Fig. 7D). If CXCL1 is blocked, there is less accumulation of neutrophils and less damage associated with reduced proinflammatory response; however, other chemotactic signals can compensate, resulting in neutrophil recruitment to the lungs (and in equal measure to uninjured mice) after bacterial infection with enhanced bacterial clearance (Fig. 7E). Neutrophils are necessary and sufficient for clearance of *P. aeruginosa* (24).

Altogether, we propose that, by attenuating, but not deleting, neutrophil numbers by CXCL1 blockade, we can prevent the early damage caused by neutrophils and, we hypothesize, bolster bacterial clearance by enhancing other mechanisms of immune chemotaxis. Indeed, we uncovered subsets of soluble mediators that were significantly and differentially altered by CXCL1 blockade after injury. One subset, represented by IL-6, IL-1β, and IL-16, was significantly decreased early (24 h) after inhalation injury. These mediators have been associated with proinflammatory shock, and their reduction may reflect reduction in neutrophils numbers and associated lung damage. IL-6 and IL-1β have been well studied in the context of burn injury, with increased levels in serum and BALF correlating well with poor clinical outcomes because of opportunistic infection (1, 11, 13, 16, 17, 19, 20). IL-16 is a cytokine released by a variety of cells (including epithelial cells) that acts as a chemoattrac-

tant for CD4$^+$ immune cells such as T-helper cells, monocytes, macrophages, and dendritic cells. Pulmonary epithelial-derived CXCL5 has been shown to be critical for neutrophil-mediated destructive inflammation in pulmonary infections (35). Reduction of these mediators after anti-CXCL1 treatment may be responsible for the decreased recruitment of neutrophils and associated lung damage after injury. In contrast, CCL25 (TECK), chemotactic for macrophages, and dendritic cells and CXCL13, chemotactic for B cells during lung infections (23), were significantly elevated 48–72 h after injury in anti-CXCL1-treated mice compared with isotype-treated controls. We hypothesize that these mediators are responsible for increased (or restoration of) chemotaxis upon secondary bacterial challenge, which aids in bacterial clearance of infection. This may be by virtue of more surviving secretory cells after the reduction in lung damage or the nature of the stimulus (e.g., DAMPS vs. pathogen-associated molecular patterns). Further study of these mediators and their inducers in the lung in response to inhalation injury and secondary bacterial infection is warranted.

A significant clinical challenge in the field of trauma has been how to suppress immune pathology without amplifying patient susceptibility to infection. What we show here is that attenuating early recruitment of neutrophils, when bacterial infection has not yet emerged, protects the lung from injury without preventing responses required to combat subsequent infection. Future studies would benefit from implementing larger animals such as sheep or pigs who can be placed on life support and used to measure clinical parameters that are vital to monitoring and improving patient outcomes. Because the current study is limited to injuries from which mice can recover without supplemental oxygen, future studies in larger animals using life support strategies can determine whether mechanisms and interventions outlined herein are applicable to more severe injuries.

In summary, our studies present and describe a novel mouse model of inhalation injury that more closely mimics inhalation injury resulting from forest and/or house fires more effectively than existing cotton smoke inhalation models. We have used this experimental model to obtain well-defined temporal relationships between DAMPs, chemokines, cytokines, and innate immune cell recruitment as well as susceptibility to opportunistic infections observed in patients with inhalational injury. We used this model to probe two key mechanisms associated with the clinical observations, describing the complementary and divergent roles of Nos2 and CXCL1. Together these and previously published data illustrate the importance of using relevant preclinical models to distinguish between inflammation, immunopathology, and protective immunity. This model will improve the ability to differentiate between correlative and causative relationships in inhalational injury. The studies presented here demonstrate that it is possible, using translationally relevant models, to uncouple clinical phenotypes from outcomes and therefore identify the most effective intervention strategies.

DISCLOSURES

No conflicts of interest, financial or otherwise, are declared by the authors.

AUTHOR CONTRIBUTIONS

J.L.D., C.M.D., R.M., and B.A.C. conceived and designed research; J.L.D., L.B.K., W.H.S., L.I.G., and M.M.M. performed experiments; J.L.D., L.B.K., and W.H.S. analyzed data; J.L.D., W.H.S., S.J., C.M.D., R.M., and B.A.C. interpreted results of experiments; J.L.D. and L.B.K. prepared figures; J.L.D., W.H.S., and R.M. drafted manuscript; J.L.D., L.B.K., C.M.D., and R.M. edited and revised manuscript; J.L.D., L.B.K., W.H.S., L.I.G., M.M.M., S.J., C.M.D., R.M., and B.A.C. approved final version of manuscript.

REFERENCES

1. **Abdel-Hafez NM, Saleh Hassan Y, El-Metwally TH.** A study on biomarkers, cytokines, and growth factors in children with burn injuries. *Ann Burns Fire Disasters* 20: 89–100, 2007.

2. **Ahn CS, Maitz PK.** The true cost of burn. *Burns* 38: 967–974, 2012. doi:10.1016/j.burns.2012.05.016.

3. **Armstrong R.** The physiological role and pharmacological potential of nitric oxide in neutrophil activation. *Int Immunopharmacol* 1: 1501–1512, 2001. doi:10.1016/S1567-5769(01)00094-7.

4. **Bogdan C.** Nitric oxide and the immune response. *Nat Immunol* 2: 907–916, 2001. doi:10.1038/ni1001-907.

5. **Buchanan IBMR, Maile R, Frelinger JA, Fair JH, Meyer AA, Cairns BA.** The effect of burn injury on CD8+ and CD4+ T cells in an irradiation model of homeostatic proliferation. *J Trauma* 61: 1062–1068, 2006. doi:10.1097/01.ta.0000195984.56153.21.

6. **Cairns B, Maile R, Barnes CM, Frelinger JA, Meyer AA.** Increased Toll-like receptor 4 expression on T cells may be a mechanism for enhanced T cell response late after burn injury. *J Trauma* 61: 293–298, 2006. doi:10.1097/01.ta.0000228969.46633.bb.

7. **Cairns BA, Barnes CM, Mlot S, Meyer AA, Maile R.** Toll-like receptor 2 and 4 ligation results in complex altered cytokine profiles early and late after burn injury. *J Trauma* 64: 1069–1077, 2008. doi:10.1097/TA.0b013e318166b7d9.

8. **Carraway MS, Piantadosi CA, Jenkinson CP, Huang Y-CT.** Differential expression of arginase and iNOS in the lung in sepsis. *Exp Lung Res* 24: 253–268, 1998. doi:10.3109/01902149809041533.

9. **Copeland S, Warren HS, Lowry SF, Calvano SE, Remick D; Inflammation and the Host Response to Injury Investigators.** Acute inflammatory response to endotoxin in mice and humans. *Clin Diagn Lab Immunol* 12: 60–67, 2005. doi:10.1128/CDLI.12.1.60-67.2005.

10. **Davis CS, Albright JM, Carter SR, Ramirez L, Kim H, Gamelli RL, Kovacs EJ.** Early pulmonary immune hyporesponsiveness is associated with mortality after burn and smoke inhalation injury. *J Burn Care Res* 33: 26–35, 2012. doi:10.1097/BCR.0b013e318234d903.

11. **Devaraj S, Venugopal SK, Singh U, Jialal I.** Hyperglycemia induces monocytic release of interleukin-6 via induction of protein kinase c-alpha and -beta. *Diabetes* 54: 85–91, 2005. doi:10.2337/diabetes.54.1.85.

12. **Dong H, Li J, Lv Y, Zhou Y, Wang G, Hu S, He X, Yang P, Zhou Z, Xiang X, Wang CY.** Comparative analysis of the alveolar macrophage proteome in ALI/ARDS patients between the exudative phase and recovery phase. *BMC Immunol* 14: 25, 2013. doi:10.1186/1471-2172-14-25.

13. **Drost AC, Burleson DG, Cioffi WG Jr, Jordan BS, Mason AD Jr, Pruitt BA Jr.** Plasma cytokines following thermal injury and their relationship with patient mortality, burn size, and time postburn. *J Trauma* 35: 335–339, 1993. doi:10.1097/00005373-199309000-00001.

14. **Dunn JL, Hunter RA, Gast K, Maile R, Cairns BA, Schoenfisch MH.** Direct detection of blood nitric oxide reveals a burn-dependent decrease of

nitric oxide in response to *Pseudomonas aeruginosa* infection. *Burns* 42: 1522–1527, 2016. doi:10.1016/j.burns.2016.05.005.

15. **Esechie A, Kiss L, Olah G, Horváth EM, Hawkins H, Szabo C, Traber DL.** Protective effect of hydrogen sulfide in a murine model of acute lung injury induced by combined burn and smoke inhalation. *Clin Sci (Lond)* 115: 91–97, 2008. doi:10.1042/CS20080021.

16. **Finnerty CC, Jeschke MG, Herndon DN, Gamelli R, Gibran N, Klein M, Silver G, Arnoldo B, Remick D, Tompkins RG; Investigators of the Inflammation and the Host Response Glue Grant.** Temporal cytokine profiles in severely burned patients: a comparison of adults and children. *Mol Med* 14: 553–560, 2008. doi:10.2119/2007-00132.Finnerty.

17. **Gauglitz GG, Finnerty CC, Herndon DN, Mlcak RP, Jeschke MG.** Are serum cytokines early predictors for the outcome of burn patients with inhalation injuries who do not survive? *Crit Care* 12: R81, 2008. doi:10.1186/cc6932.

18. **Gross D, Loftus JJ, Robertson AF.** Method for measuring smoke from burning materials. *Am Soc Testing Mats* 422: 1967. doi:10.1520/STP41310S.

19. **Hur J, Yang HT, Chun W, Kim JH, Shin SH, Kang HJ, Kim HS.** Inflammatory cytokines and their prognostic ability in cases of major burn injury. *Ann Lab Med* 35: 105–110, 2015. doi:10.3343/alm.2015.35.1.105.

20. **Jawa RS, Anillo S, Huntoon K, Baumann H, Kulaylat M.** Interleukin-6 in surgery, trauma, and critical care part II: clinical implications. *J Intensive Care Med* 26: 73–87, 2011. doi:10.1177/0885066610384188.

21. **Johnson ER, Matthay MA.** Acute lung injury: epidemiology, pathogenesis, and treatment. *J Aerosol Med Pulm Drug Deliv* 23: 243–252, 2010. doi:10.1089/jamp.2009.0775.

22. **Jones SW, Zhou H, Ortiz-Pujols SM, Maile R, Herbst M, Joyner BL Jr, Zhang H, Kesic M, Jaspers I, Short KA, Meyer AA, Peden DB, Cairns BA, Noah TL.** Bronchoscopy-derived correlates of lung injury following inhalational injuries: a prospective observational study. *PLoS One* 8: e64250, 2013. doi:10.1371/journal.pone.0064250.

23. **Khader SA, Guglani L, Rangel-Moreno J, Gopal R, Junecko BA, Fountain JJ, Martino C, Pearl JE, Tighe M, Lin YY, Slight S, Kolls JK, Reinhart TA, Randall TD, Cooper AM.** IL-23 is required for long-term control of Mycobacterium tuberculosis and B cell follicle formation in the infected lung. *J Immunol* 187: 5402–5407, 2011. doi:10.4049/jimmunol.1101377.

24. **Koh AY, Priebe GP, Ray C, Van Rooijen N, Pier GB.** Inescapable need for neutrophils as mediators of cellular innate immunity to acute *Pseudomonas aeruginosa* pneumonia. *Infect Immun* 77: 5300–5310, 2009. doi:10.1128/IAI.00501-09.

25. **Lange M, Hamahata A, Traber DL, Connelly R, Nakano Y, Traber LD, Schmalstieg FC, Herndon DN, Enkhbaatar P.** Pulmonary microvascular hyperpermeability and expression of vascular endothelial growth factor in smoke inhalation- and pneumonia-induced acute lung injury. *Burns* 38: 1072–1078, 2012. doi:10.1016/j.burns.2012.02.019.

26. **Lange M, Szabo C, Traber DL, Horvath E, Hamahata A, Nakano Y, Traber LD, Cox RA, Schmalstieg FC, Herndon DN, Enkhbaatar P.** Time profile of oxidative stress and neutrophil activation in ovine acute lung injury and sepsis. *Shock* 37: 468–472, 2012. doi:10.1097/SHK.0b013e31824b1793.

27. **Liu F, Li W, Pauluhn J, Trübel H, Wang C.** Rat models of acute lung injury: exhaled nitric oxide as a sensitive, noninvasive real-time biomarker of prognosis and efficacy of intervention. *Toxicology* 310: 104–114, 2013. doi:10.1016/j.tox.2013.05.016.

28. **Maile R, Barnes CM, Nielsen AI, Meyer AA, Frelinger JA, Cairns BA.** Lymphopenia-induced homeostatic proliferation of CD8+ T cells is a mechanism for effective allogeneic skin graft rejection following burn injury. *J Immunol* 176: 6717–6726, 2006. doi:10.4049/jimmunol.176.11.6717.

29. **Maile R, Jones S, Pan Y, Zhou H, Jaspers I, Peden DB, Cairns BA, Noah TL.** Association between early airway damage-associated molecular patterns and subsequent bacterial infection in patients with inhalational and burn injury. *Am J Physiol Lung Cell Mol Physiol* 308: L855–L860, 2015. doi:10.1152/ajplung.00321.2014.

30. **Matthew E, Warden G, Dedman J.** A murine model of smoke inhalation. *Am J Physiol Lung Cell Mol Physiol* 280: L716–L723, 2001. doi:10.1152/ajplung.2001.280.4.L716.

31. **Matute-Bello G, Downey G, Moore BB, Groshong SD, Matthay MA, Slutsky AS, Kuebler WM; Acute Lung Injury in Animals Study Group.** An official American Thoracic Society workshop report: features and measurements of experimental acute lung injury in animals. *Am J Respir Cell Mol Biol* 44: 725–738, 2011. doi:10.1165/rcmb.2009-0210ST.

32. **Mendoza AENC, Neely CJ, Charles AG, Kartchner LB, Brickey WJ, Khoury AL, Sempowski GD, Ting JP, Cairns BA, Maile R.** Radiation combined with thermal injury induces immature myeloid cells. *Shock* 38: 532–542, 2012. doi:10.1097/SHK.0b013e31826c5b19.

33. **Mizutani A, Enkhbaatar P, Esechie A, Traber LD, Cox RA, Hawkins HK, Deyo DJ, Murakami K, Noguchi T, Traber DL.** Pulmonary changes in a mouse model of combined burn and smoke inhalation-induced injury. *J Appl Physiol (1985)* 105: 678–684, 2008. doi:10.1152/japplphysiol.00232.2007.

34. **Neely CJ, Kartchner LB, Mendoza AE, Linz BM, Frelinger JA, Wolfgang MC, Maile R, Cairns BA.** Flagellin treatment prevents increased susceptibility to systemic bacterial infection after injury by inhibiting anti-inflammatory IL-10+ IL-12- neutrophil polarization. *PLoS One* 9: e85623, 2014. doi:10.1371/journal.pone.0085623.

35. **Nouailles G, Dorhoi A, Koch M, Zerrahn J, Weiner J III, Faé KC, Arrey F, Kuhlmann S, Bandermann S, Loewe D, Mollenkopf HJ, Vogelzang A, Meyer-Schwesinger C, Mittrücker HW, McEwen G, Kaufmann SH.** CXCL5-secreting pulmonary epithelial cells drive destructive neutrophilic inflammation in tuberculosis. *J Clin Invest* 124: 1268–1282, 2014. doi:10.1172/JCI72030.

36. **Plackett TP, Gamelli RL, Kovacs EJ.** Gender-based differences in cytokine production after burn injury: a role of interleukin-6. *J Am Coll Surg* 210: 73–78, 2010. doi:10.1016/j.jamcollsurg.2009.09.019.

37. **Rehberg S, Maybauer MO, Enkhbaatar P, Maybauer DM, Yamamoto Y, Traber DL.** Pathophysiology, management and treatment of smoke inhalation injury. *Expert Rev Respir Med* 3: 283–297, 2009. doi:10.1586/ers.09.21.

38. **Reiss LK, Uhlig U, Uhlig S.** Models and mechanisms of acute lung injury caused by direct insults. *Eur J Cell Biol* 91: 590–601, 2012. doi:10.1016/j.ejcb.2011.11.004.

39. **Soejima K, Traber LD, Schmalstieg FC, Hawkins H, Jodoin JM, Szabo C, Szabo E, Virag L, Salzman A, Traber DL.** Role of nitric oxide in vascular permeability after combined burns and smoke inhalation injury. *Am J Respir Crit Care Med* 163: 745–752, 2001. doi:10.1164/ajrccm.163.3.9912052.

40. **Vindenes H, Ulvestad E, Bjerknes R.** Increased levels of circulating interleukin-8 in patients with large burns: relation to burn size and sepsis. *J Trauma* 39: 635–640, 1995. doi:10.1097/00005373-199510000-00003.

41. **Wurtz R, Karajovic M, Dacumos E, Jovanovic B, Hanumadass M.** Nosocomial infections in a burn intensive care unit. *Burns* 21: 181–184, 1995. doi:10.1016/0305-4179(95)80005-9.

42. **Zawacki BE, Jung RC, Joyce J, Rincon E.** Smoke, burns, and the natural history of inhalation injury in fire victims: a correlation of experimental and clinical data. *Ann Surg* 185: 100–110, 1977.

43. **Zheng H, Chen XL, Han ZX, Zhang Z, Wang SY, Xu QL.** Ligustrazine attenuates acute lung injury after burn trauma. *Burns* 31: 453–458, 2005. doi:10.1016/j.burns.2004.10.023.